Zagazig University Medical Journal
www.zumj.journals.ekb.eg
Volume 29, Issue 1, January 2023, Page (257-265) Supplement Issue

Manuscript ID ZUMJ-2208-2621 (R1)

DOI **10.21608/zumj.2022.155920.2621**

ORIGINAL ARTICLE

Can MSCT be a Useful Tool to Orthopedic Surgeons in Assessment of The Morphology of The PM (Posterior Malleolus) Fractures Using Bartonicek-Rammelt Classification?

Dena Abd El Aziz El Sammak*[1], Ahmed Mohamed Alsowey[1], Mai E.M khamis[1]

Radiodiagnosis Department, Zagazig University Hospital, Zagazig, Egypt

***Corresponding author:**
Dena Abd El Aziz El Sammak
Radiodiagnosis Department,
Zagazig University Hospital,
Egypt

E-mail:
denaelsammak@gmail.com

Submit Date 2022-08-29
Revise Date 2022-09-30
Accept Date 2022-11-04

ABSTRACT

Background: The posterior tibio-fibular ligament is attached to the PM, thus if the PM is affected, disruption of the ankle congruency develops. Plain radiography provides insufficient evaluation of the pathoanatomy of the PM fragment. However, MSCT images determine the accurate morphology of the PM fracture, thus all patients with ankle fractures should be assessed by preoperative MSCT imaging.

The aim of this study was to assess: (1) the morphological characteristics of the PM fragment, (2) the correlation between the fragment height (FH), the affected articular surface area, the fragment area ratio (FAR) and the fragment length ratio (FLR), (3) the relationship between the FH and the occurrence of die-punch.

Methods: This study was retrospective, included 85 patients, 34 were men (40%) and 51 were women (60%), mean age was 52.38±16.25 years. Patients who underwent surgery for a unilateral ankle fracture involving a PM fracture were included in this study. All patients underwent plain radiography including AP, lateral and AP mortise views of both ankles, and MSCT with axial, sagittal, coronal planes and 3D reconstruction.

Results: 76.5% were trimalleolar fractures, 23.5% were bimalleolar fractures, no isolated PM fractures. Weber type B fractures were the most common, occurred in 68.2%. The most common Lauge-Hansen classification was a supination external rotation stage IV fracture (44.7%). The FH correlated positively with the fracture area, as well as the FAR, and the FLR. The mean FH increased in the positive die punch group. Type II PM fractures were the most common occurred in 47.1%.

Conclusion: Preoperative assessment of the FH, area, FLR and FAR with MSCT imaging can help the orthopedic surgeons in determining the appropriate surgical approach, thus restoring the syndesmotic stability, and ultimately improving the functional outcomes.

Keywords: MSC; Posterior malleolus; Fractures,Bartonicek-Rammelt classification

INTRODUCTION

Ankle fractures account for 3.9% of all fractures, with an incidence rate 187 per 100,000 person each year **(1)**. Isolated PM fractures are scarce, occurred in 0.5%-1% of ankle fractures. However, trimalleolar fractures including PM occurred in 7% to 44% **(2)**. The posterior tibio-fibular ligament is attached to the PM, thus if the PM is affected, disruption of the ankle congruency develops. Also, poor outcome and traumatic arthritis will occur, ankle fractures with PM involvement have a 30 percent higher rate of traumatic arthritis **(3)**.

The classification systems of PM fractures are: AO, Heim, Haraguchi, and Bartonicek-Rammelt. The 1st two systems depend on plain radiography, while the latter two systems based on MSCT images. Plain radiography provides insufficient evaluation of the pathoanatomy of the PM fragment. However, MSCT images determine the accurate shape of the PM fracture, thus, all patients with ankle fractures should be assessed by preoperative MSCT imaging **(4).**

In 2006, Haraguchi et al. analyzed the cross-sectional MSCT images only, and did not perform 2D or 3D reconstruction. However, Bartoníček et al. suggested a new classification depending on 3D MSCT reconstruction in 2015 **(5).**

There are multiple criteria for surgical fixation of a PM fragment which are; fragment size equals 1/4 to 1/3 of the articular surface, greater than 2 mm displacement, incisura involvement, the presence of intercalary fragments, plafond impaction, and syndesmotic instability **(6).** The posterolateral and

posteromedial approaches to the ankle joint and their modifications allow an anatomic reduction, stable fixation and restoring the tibiofibular mortise **(7).** The aim of this study was to evaluate**: (a)** the morphological characteristics of the PM fragment, **(b)** the correlation between the FH, the fracture area, the FAR and the FLR, **(c)** the relationship between the FH and the die-punch fracture.

METHODS

Patient characteristics

This study was a retrospective study, done in the radio-diagnosis department of Zagazig University Hospital. The study included 85 patients, 34 were male (40%) and 51 were female (60%), mean age was 52.38±16.25 years, ranging from 19 to 75 years, referred from orthopedic surgery department in Zagazig University Hospital during the period from November 2021 to June 2022.

Patients who underwent surgery for a unilateral ankle fracture involving a PM fracture were included in this study.

Exclusion criteria were: 1) pathological fractures, 2) patients aged less than 18 years, 3) pilon fractures, 4) ipsilateral ankle congenital deformity, 5) concomitant fractures of the same limb and polytraumatized patients.

All patients underwent plain radiography including AP, lateral and AP mortise views of both ankles, and MSCT with axial, sagittal, coronal planes and 3D reconstruction. The included patients gave their written informed consent, and the protocol of this study was approved by the research ethical committee of Faculty of Medicine, Zagazig University. The study was done according to the Code of Ethics of the World Medical Association (Declaration of Helsinki) for studies involving humans.

MSCT Technique

Multislice CT (MSCT) was done in axial cuts from the mid/distal third of the leg to the bottom of the calcaneus on 128-slice CT scanner (Philips ingenuity 128), using the following parameters: 128x1 mm detector row configuration, 1.25 mm slice thickness, 1 mm collimation, 1 mm reconstruction interval, 1.375 pitch, 300 mAs, 120 kVp. Standard bone window 3000/300 (WW/WL). Standard soft tissue window 400/50 (WW/WL).

Post processing Technique

Multiplanar reformatted images (MPR) were acquired using the machine software in coronal and sagittal planes. The thin axial slices were transmitted directly from the MSCT scanner to a workstation for reconstruction of 3D images which were important adjuncts to 2D images.

Interpretation

A) Morphological characteristics of PM fragment:

According to Bartonicek classification **(8)**, PM fractures are classified into:

Type I: extra-incisural fragment, an intact fibular notch

Type II: a postero-lateral fragment extends into the fibular notch

Type III: a postero-medial two-part fragment involves the medial malleolus

Type IV: a large postero-lateral triangular fragment involves > 1/3 of the fibular notch

B) Measurements:

Axial MSCT images aid in measuring the FLR and the FAR. The length of the fragment (l) is the distance between the apex of the fragment and the posterior tibial lip. The capital diameter of the tibial plafond (L) is measured between the anterior and posterior tibial lips. The ratio between the fragment length (l) and the capital diameter of the tibial plafond (L) is called the **FLR**.

The **FAR** is calculated by measuring the posterior fragment area (s) and the remaining cross-sectional area of the tibia (S) at the level of the tibial plafond. The **FAR** is defined as the ratio of the fragment area (s) to the total cross sectional area of the tibial plafond (s+S).

The **FH** is measured on the sagittal MSCT image. We identify a neutral axis (NA) based on the bisection of the mid shaft of the tibia, the **FH** is defined as the largest distance from the apex of the fragment to the point that is across the joint and the neutral axis (NA).

STATISTICAL ANALYSIS

All data were collected, tabulated and statistically analyzed using SPSS 22.0 for windows (IBM Inc., Chicago, IL, USA). Continuous quantitative variables were expressed as the mean ± SD & median (range), and categorical qualitative variables were expressed as an absolute frequencies (number) & relative frequencies (percentage).

RESULTS

Demographic characteristics of 85 patients with PM fractures (Table 1)

A total of 85 patients, 34 males (40%) and 51females (60%), aged 19-75 years, mean age

52.38 ± 16.25 years, were included in this study. The right ankle was affected in 42.4% and the left ankle in 57.6%.

The most common causes of PM fractures were due to fall from a standing height in 50 patients (58.8%), and twisted ankle in 20 patients (23.5%).

6 patients (7.1%) suffered from open fractures. 37 patients (43.5%) presented with a fracture dislocation of the ankle.

Multiple comorbidities were noted in this study as, arterial hypertension (69.4%), diabetes mellitus (15.3%), osteoporosis (11.8%), peripheral arterial occlusive disease (2.4%), and rheumatoid arthritis (1.2%).

65 fractures were trimalleolar (76.5%), 20 fractures were bimalleolar (23.5%), no isolated PM fractures.

Weber B fractures occurred in 68.2%, Weber C fractures existed in 31.8%, Weber A fractures were not detected in this study.

11.8% had pronation abduction stage III (PA-III) fractures, 20% pronation external rotation stage IV (PER-IV) fractures, 23.5% supination external rotation stage III (SER-III) fractures, and 44.7% supination external rotation stage IV (SER-IV) fractures. No supination adduction fractures were seen in this study.

The mean height of the PM fragment was 21.11±9.20 mm, and the mean fracture area was 297.01± 219.27mm^2. The mean FAR was 11.68±3.58%, and the mean FLR was 26.42± 2.86 %.

As shown in Table 2, the FH correlated positively with the fracture area**,** the FAR and the FLR with correlation coefficients of 0.819, 0.833 and 0.817, respectively ($p < 0.001$).

Die-punch was detected in 47 cases (55.3%). The mean FH was larger in the positive die punch group (28.44±4.37 mm) than in the negative die punch group (12.06±4.01 mm) **as shown in Table 3**.

Type II PM fractures were the most common type, seen in 40 patients (47.1%). However type III, type IV and type I were seen in 32.9%, 18.8%, and 1.2%, respectively.

As shown in Table 4, intercalary fragments were detected in 30 patients (35.3%); most common in type III PM fractures (22 patients), less frequently in type II (6 patients) and type IV (2 patients). Intercalary fragments were not detected in type I PM fractures. Female preponderance was seen in type III (7 men vs. 21 women) and type IV PM fractures (2 men vs. 14 women).

Table (1): Patient & Fracture characteristics in 85 ankle fractures**.**

Patient & Fracture characteristics	Ankle fractures (N=85)		Patient & Fracture characteristics	Ankle fractures (N=85)	
	Number	Percent		Number	Percent
Sex			**Die punch**		
Male	**34**	**40%**	**Absent**	**38**	**44.7%**
Female	**51**	**60%**	**Present**	**47**	**55.3%**
Age (years)			**Fragment height (mm)**		
Mean±SD	**52.38±16.25**		**Mean±SD**	**21.11±9.20**	
Median (Range)	**55 (19 – 75)**		**Median (Range)**	**22.63 (6.20 – 36.13)**	
Fracture dislocation			**Fracture area (mm^2)**		
Absent	**48**	**56.5%**	**Mean±SD**	**297.01±219.27**	
Present	**37**	**43.5%**	**Median (Range)**	**220 (80 – 665)**	
Open fracture			**FAR (%)**		
Absent	**79**	**92.9%**	**Mean±SD**	**11.68±3.58**	
Present	**6**	**7.1%**	**Median (Range)**	**10.90 (7.20 – 18.60**	
Side of injury			**FLR (%)**		
Right	**36**	**42.4%**	**Mean±SD**	**26.42±2.86**	
Left	**49**	**57.6%**	**Median (Range)**	**26.30 (22.50 – 31.80)**	
Intercalary fragment			**Danis-Weber classification**		
Absent	**55**	**64.7%**	**Weber A**	**0**	**0%**
Present	**30**	**35.3%**	**Weber B**	**58**	**68.2%**
			Weber C	**27**	**31.8%**

Patient & Fracture characteristics	Ankle fractures (N=85)		Patient & Fracture characteristics	Ankle fractures (N=85)	
	Number	Percent		Number	Percent
Mechanism of injury			Lauge-Hansen classification		
Fall from standing height	50	58.8%	SA	0	0%
Twisted ankle	20	23.5%	SER-3	20	23.5%
Fall from height >2m	7	8.2%	SER-4	38	44.7%
Road traffic collision	6	7.1%	PER-4	17	20%
Fall from motorbike	2	2.4%	PA-3	10	11.8%
Co-morbidities			Bartonicek Type		
Arterial hypertension	59	69.4%	Type 1	1	1.2%
Diabetes mellitus	13	15.3%	Type 2	40	47.1%
Osteoporosis	10	11.8%	Type 3	28	32.9%
PAOD	2	2.4%	Type 4	16	18.8%
Rheumatoid arthritis	1	1.2%			
Types of PM fracture					
Isolated	0	0%			
Bimalleolar	20	23.5%			
Trimalleolar	65	76.5%			

Categorical variables were expressed as number (percentage); Continuous variables were expressed as mean ± SD & median (range).

Table (2): Correlation between fragment height, fracture area and fragment area ratio (FAR).

		Fracture area (mm^2)	Fragment area ratio (FAR) (%)	Fragment length ratio (FLR) (%)
Fragment height (mm)	r	+0.819	+0.833	+0.817
	p-value	<0.001	<0.001	<0.001
Fracture area (mm^2)	r		+0.830	+0.760
	p-value		<0.001	<0.001
Fragment area ratio (FAR) (%)	r			+0.793
	p-value			<0.001

Table (3): PM fragment height stratified by Die-punch

Die punch	N	Fragment height			
		Mean	±SD	Median	(Range)
Absent	38	12.06	4.01	11.1050	(6.20 – 19.59)
Present	47	28.44	4.37	28.3200	(20.23 – 36.13)

Continuous variables were expressed as mean ± SD & median (range).

Table (4): PMF morphology assessment using Bartonicek-Rammelt classification**.**

	All patients (N=85)		Bartonicek Type							
			Type 1 (N=1)		Type 2 (N=40)		Type 3 (N=28)		Type 4 (N=16)	
	No.	%	No.	%	No.	%	No.	%	No.	%
Sex										
Male	34	40%	1	2.9%	24	70.6%	7	20.6 %	2	5.9%
Female	51	60%	0	0%	16	31.4%	21	41.2 %	14	27.5%
Intercalary fragment										
Absent	55	64.7 %	1	100 %	34	85%	6	21.4 %	14	87.5%

	All patients (N=85)		Bartonicek Type									
			Type 1 (N=1)		Type 2 (N=40)		Type 3 (N=28)		Type 4 (N=16)			
	No.	%	No.	%	No.	%	No.	%	No.	%		
Present	**30**	**35.3 %**	**0**	**0%**	**6**	**15%**	**22**	**78.6 %**	**2**	**12.5%**		

Categorical variables were expressed as number (percentage).

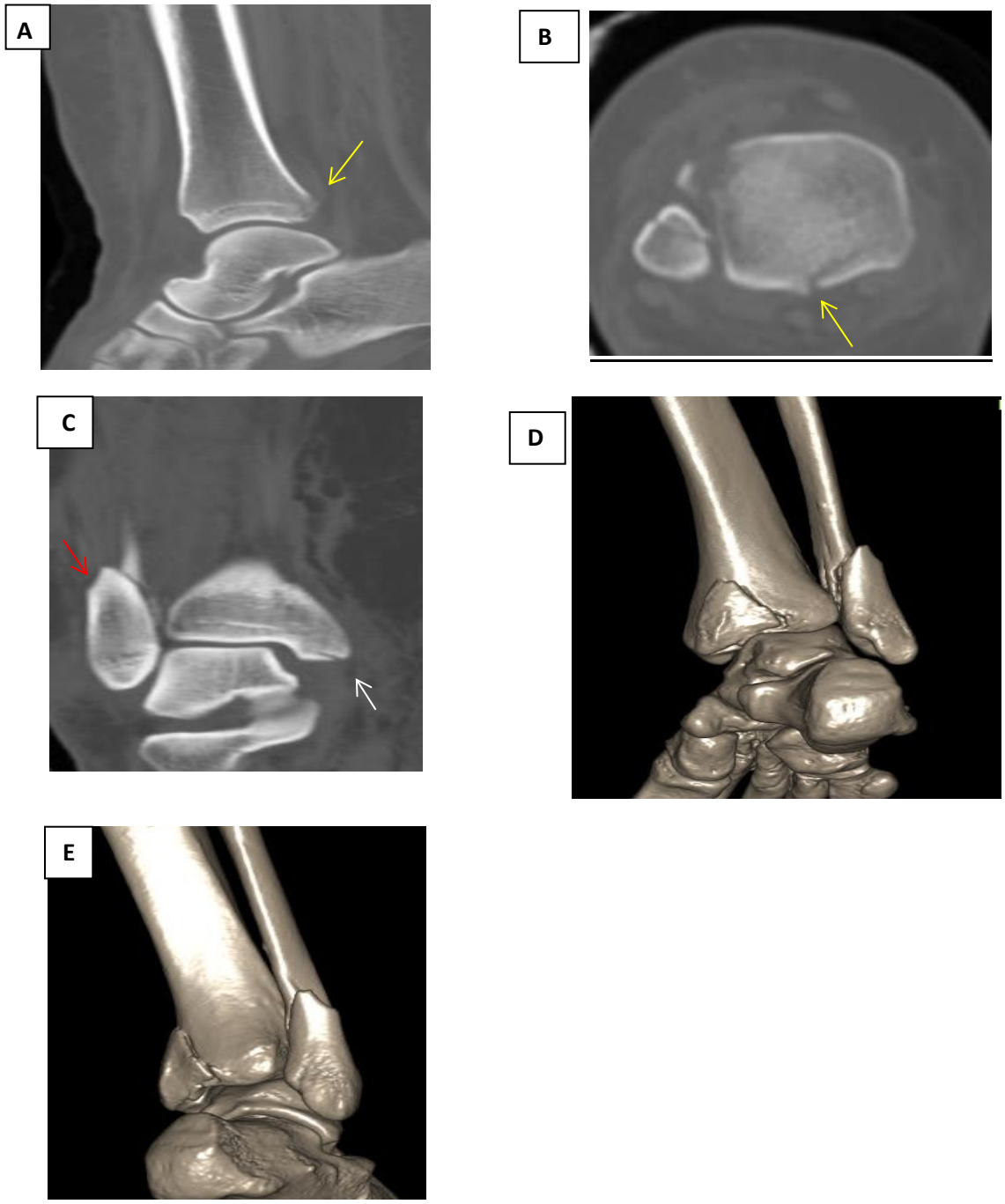

Figure (1):(A) Sagittal and (B) Axial MSCT images (bone window) show type 1 posterior malleolus fracture (yellow arrows). **(C) Coronal MSCT image (bone window)** shows medial malleolus fracture (white arrow) and high-location fibular fracture (red arrow), the fibular fracture is spiral and is located above the inferior tibio-fibular joint level. This is Weber type C fracture, and stage 4 of the pronation-external rotation type of the Lauge-Hansen classification. **(D) & (E) 3D MSCT images** confirm the previous findings

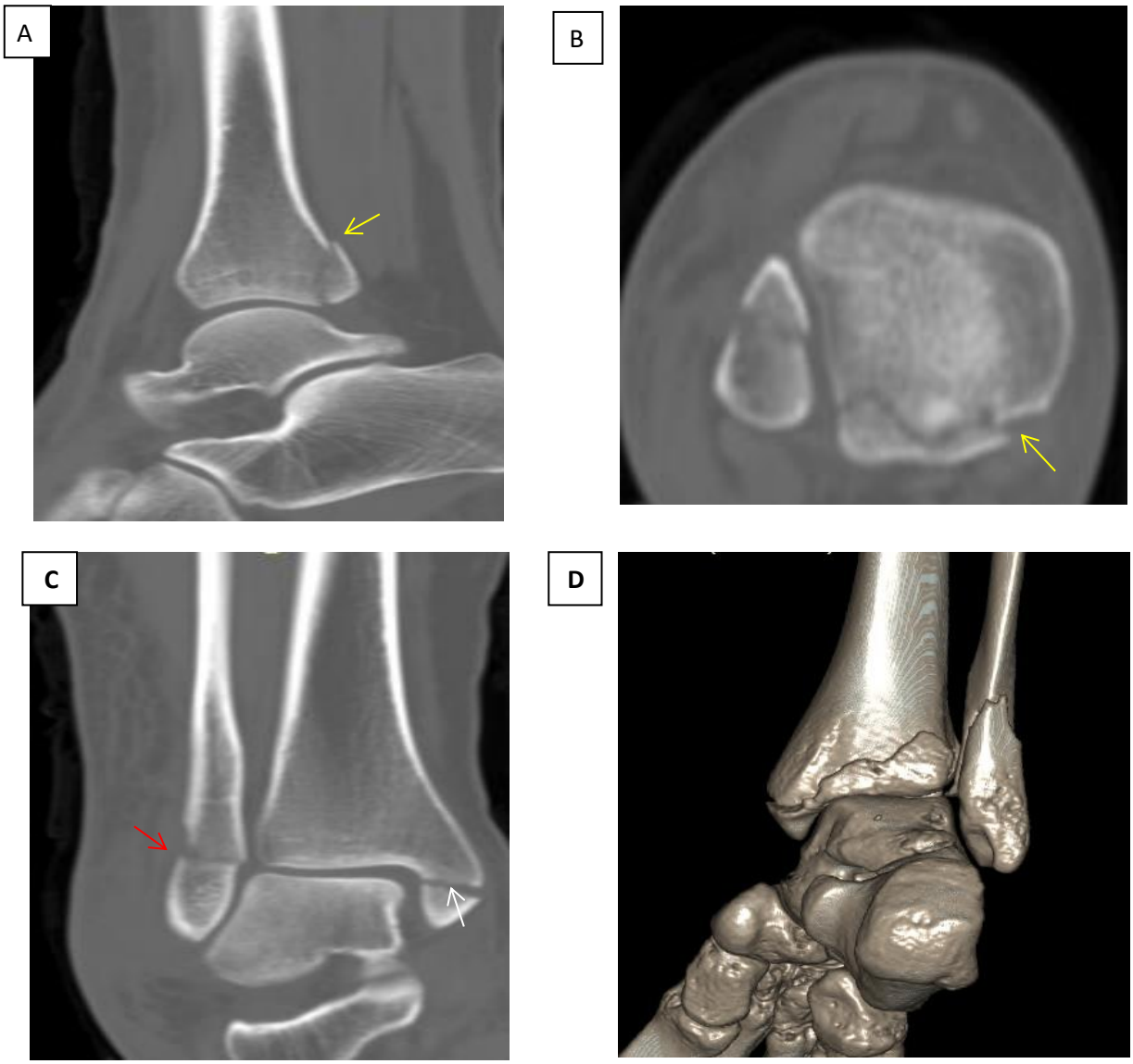

Figure (2):(A) Sagittal and (B) Axial MSCT images (bone window) show type 2 posterior malleolus fracture (yellow arrows). **(C) Coronal MSCT image (bone window)** shows lateral (red arrow) and medial (white arrow) malleoli fractures. The lateral malleolus fracture was at the inferior tibio-fibular joint level. This is Weber type B fracture or stage 4 of the supination-external rotation of the Lauge-Hansen classification. **(D) 3D MSCT image** confirms the previous findings.

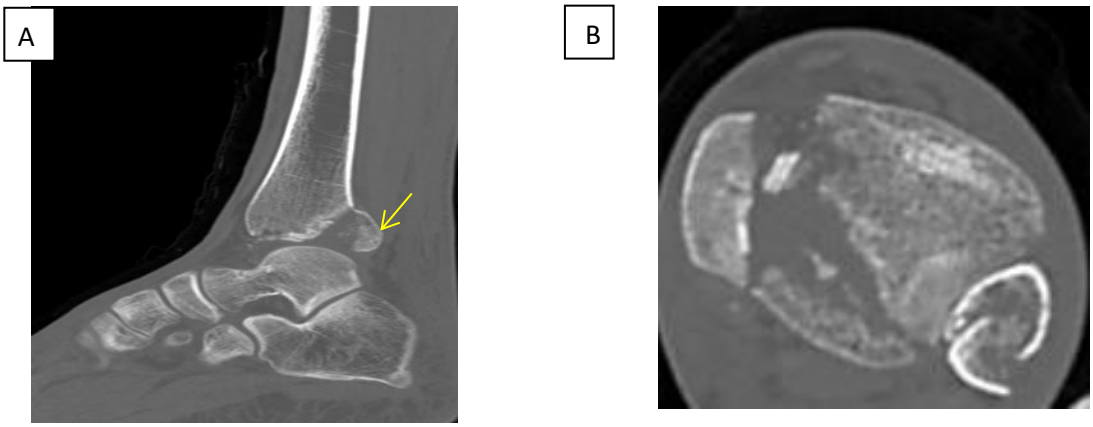

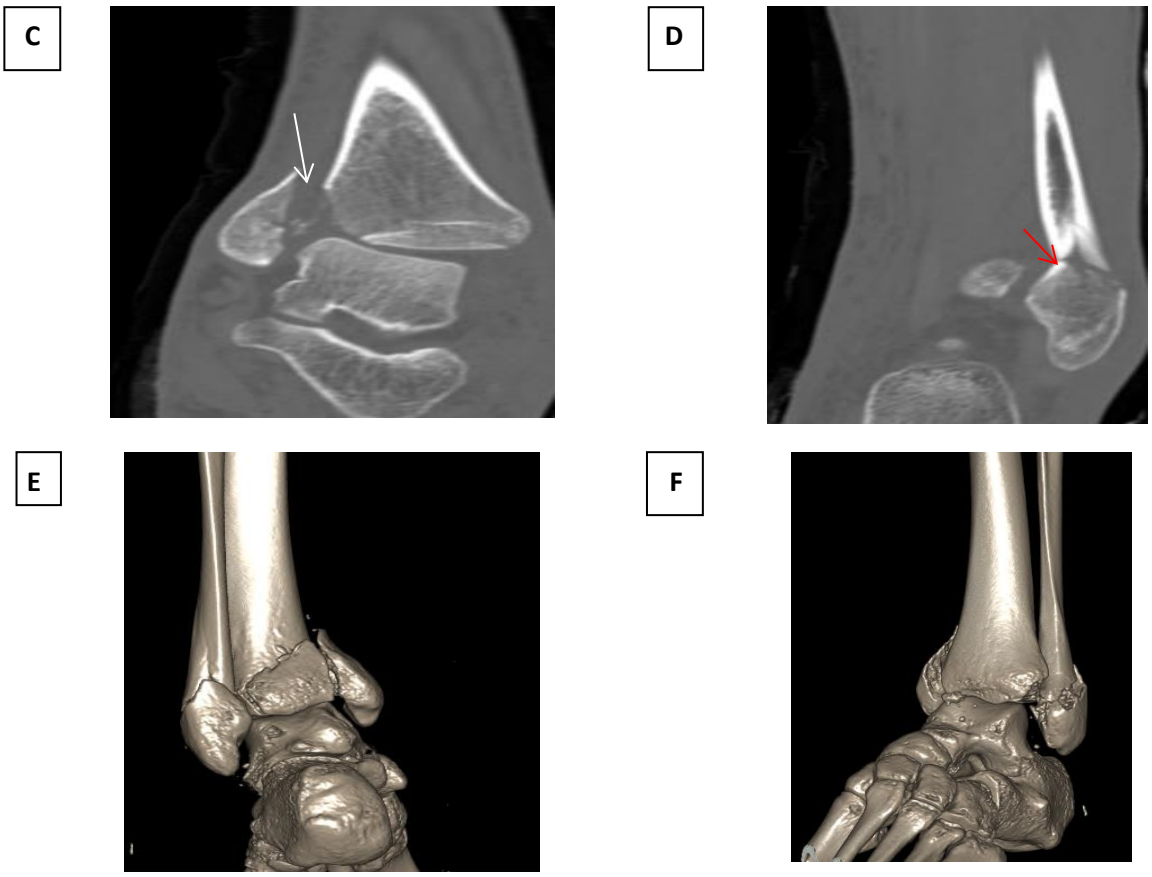

Figure (3): (A) Sagittal and (B) Axial MSCT images (bone window) show type 3 posterior malleolus fracture (yellow arrows). (C) and (D) Coronal MSCT images (bone window) show the medial malleolus fracture is vertical (white arrow) and the lateral malleolus fracture is spiral (red arrow). (E) and (F) 3D MSCT images show trimalleoli fractures. The lateral malleolus fracture is at the inferior tibio-fibular joint level. This is Weber type B and stage 4 of the supination-external rotation of the Lauge-Hansen classification.

DISSCUSION

The PM is a portion of the distal tibio-fibular complex, which aids in preserving the stability of the ankle joint **(9).** Rotation violence acts on the PM through the inferior posterior tibio-fibular ligament, the inferior tibio-fibular transverse ligament, and the joint capsule, causing avulsion fracture **(10).** Plain x-ray is poor in analyzing the size, site, and displacement of a PM fracture, due to the presence of back-slabs or splints, and the difficulty with positioning of the patient **(11).** Also, plain radiography cannot adequately detect essential features as intercalary fragments, incisura involvement and joint surface impaction **(12).**

MSCT is a useful tool to orthopedic surgeons in planning the fixation of the PM fractures, based on determining the extension pattern of the fracture, the comminution of the fibular and tibial malleoli, as well as the evaluation of the morphological characteristics of the PM fragment **(13).**

Ankle fractures with a PM component have a less satisfactory clinical outcome, and future comorbidities may occur, such as chronic pain, traumatic arthritis and instability **(14).**

A total of 85 patients, including 34 males (40%) and 51females (60%), aged 19-75 years, mean age 52.38 ± 16.25 years, were included in this study.

Palmanovich et al. (15) stated that PM fractures occur in all ages, but being commoner in elderly female patients, in whom this may represent a low-energy fragility fracture.

In this study, 50 injuries (58.8%) were due to fall from standing height and 20 injuries (23.5%) were due to twisted ankle. 6 patients (7.1%) suffered from open fractures, and 37 patients (43.5%) presented with fracture dislocations of the ankle.

Yearson et al. (16) mentioned in a study on 160 PM fractures that, most injuries were caused by a fall from standing height and not a high energy injury. 14 of 160 injuries were open fractures (8.8%), 67 of 160 patients (41.9%) had fracture dislocations of the ankle.

In this study, 65 fractures were trimalleolar (76.5%), 20 fractures were bimalleolar (23.5%), no isolated PM fractures.

Kang et al. (17) reported in their study that, 120 fractures were trimalleolar (75%), 37 fractures were bimalleolar (posterior malleolus and either

medial or lateral malleolus - 23.1%), and only 3 fractures were isolated PM fractures (1.9%).

In this study, Weber B fractures occurred in 68.2%, Weber C fractures occurred in 31.8%, Weber A fractures were not detected.

Han et al. (18) stated that the most common pattern of ankle fracture is Weber B fracture, this is a trans-syndesmotic fracture with usually partial, and less commonly total rupture of the syndesmosis. It is the result of an exo-rotation force on the supinated foot. In this study, 11.8% had pronation abduction stage III (PA-III) fractures, 20% had pronation external rotation stage IV (PER-IV) fractures, 23.5% had supination external rotation stage III (SER-III) fractures, and 44.7% had supination external rotation stage IV (SER-IV) fractures. No supination adduction fractures were seen in this study. **Tosun et al. (19)** stated that according to the Lauge-Hansen classification, the ankle may be in pronation (eversion) or supination (inversion) at the time of trauma, 3 deforming forces on the ankle may occur; abduction, adduction, and external rotation, which determine multiple mechanisms of injury as pronation-abduction, pronation external rotation, supination-adduction, and supination external rotation.

In this study, the mean FH was 21.11±9.20 mm, and the mean area was 297.01± 219.27mm^2. The mean FAR was 11.68±3.58%, and the mean FLR was 26.42± 2.86%. The FH correlated positively with the fracture area**,** the FAR and the FLR with correlation coefficients of 0.819, 0.833 and 0.817, respectively ($p < 0.001$).

Wang et al. (2) mentioned in a study on 48 patients with PM fractures that the average height of the fracture was 18.19 mm, the average area was 202.28 mm^2, and the average fracture area ratio was 17.84%, the FH correlated positively with the fracture area and FAR, with a correlation coefficient of 0.4827 and 0.4641, respectively ($p < 0.0001$).

In this study, die-punch was visible in 47 cases (55.3%). The mean FH was larger in the positive die punch group (28.44±4.37 mm) than in the negative die punch group (12.06±4.01 mm).

Die-punch is a depressed or impacted intra-articular fracture accompanied by vertical axial violence, so, if rotational violence combines with axial violence, small bone fragments will be embedded between the fracture sutures, hindering the reduction and affecting the prognosis **(20).**

In agreement with this study, **Wang et al. (2)** mentioned that the PM fractures with "die-punch" tend to have a significant greater average height than those without "die-punch.

In this study, type II PM fractures were the most common type, seen in 40 patients (47.1%). However type III, type IV and type I were seen in 32.9%, 18.8%, and 1.2%, respectively. Intercalary fragments were detected in 30 patients (35.3%); most common in type III PM fractures (22 patients), less frequently in type II (6 patients) and type IV (2 patients). Intercalary fragments were not detected in type I PM fractures. Female preponderance was seen in type III (7 men vs. 21 women) and type IV PM fractures (2 men vs. 14 women). **Rammelt and Bartonicek (21)** mentioned that most of the PM fractures are type II Bartoníček and Rammelt classification. **Tuček et al. (5)** reported a significant female preponderance for Bartoníček–Rammelt type III and IV fractures, because old females with osteoporosis are prone to severe fracture patterns. **Sultan et al. (22)** stated that intercalary fragments were seen most frequently in type II and III PM fractures, these results were similar to those mentioned by **Wang et al (2)** and **Yearson et al (16)**. There were some limitations in this study that needed to be considered. Firstly, this was designed as a retrospective study. Secondly, there was a possibility of statistical error due to the small sample size. Future prospective studies with larger sample sizes are required to confirm our results.

CONCLUSION

The morphological features of the PM fragment differ according to the ankle fracture pattern based on the injury mechanism.

Preoperative assessment of the FH, area, FLR and FAR with MSCT imaging can help the orthopedic surgeons in determining the appropriate surgical approach, thus restoring the syndesmotic stability, and ultimately improving the functional outcomes.

Declaration of interest: The authors report no conflicts of interest. The authors alone are responsible for the content and writing of the paper.

Funding information: None declared**.**

REFERENCE

1. Yi Y, Chun D, Won SH, Park S, Lee S and Cho J. Morphological characteristics of the posterior malleolar fragment according to ankle fracture patterns: a computed tomography- based study. BMC Musculoskelet Disord. 2018; 19(1):51. https://doi.org/10.1186/s12891-018-1974-1.
2. Wang Z, Yuan C, Zhu G, Geng X, Zhang C, Huang J, et al. A retrospective study on the morphology of posterior malleolar fractures based on a CT scan: whether we ignore the importance of fracture height. Biomed Res Int 2020:2903537.
3. Sánchez EV, González CO, Diezhandino AA, Morata ES, Rico JV. How to address the posterior malleolus in ankle fractures? A decision-making model based on the computerised tomography findings. Int Orthop. 2020; 44(6):1177–85. https://doi.org/10.1007/s00264-020-04481-5.
4. Neumann AP and Rammelt S. Ankle fractures involving the posterior malleolus: patient characteristics and 7 year results in 100 cases. Arch

Orthop Trauma Surg. 2021. https://doi.org/10.1007/s00402-021-03875-3.
5. Tuček M, Rammelt S, Kostlivy K, Bartoniček J. CT controlled results of direct reduction and fixation of posterior malleolus in ankle fractures. Eur J Trauma Emerg Surg. 2021; 47(4):913-20. doi: 10.1007/s00068-020-01309-0 .
6. Maluta T, Samaila E, Amarossi A, Dorigotti A, Ricci M, Vecchini E, et al. Can treatment of posterior malleolus fractures with tibio-fibular instability be usefully addressed by Bartonicek classification? Foot Ankle Surg. 2022; 28(1):126-33. https:// doi. org/ 10. 1016/j. fas. 2021. 02. 009.
7. Mittlmeier T, Sas M, Randow M, Wichelhaus A. Fracture of the posterior malleolus: a paradigm shift. Unfallchirurg 2021; 124(3):181–9. doi: 10.1007/s00113-021-00954-3.
8. Bartoniček J, Rammelt S, Kostlivy K, Vaněček V, Klika D, Trešl I .Anatomy and classification of the posterior tibial fragment in ankle fractures. Arch Orthop Trauma Surg 2015 ;135(4):505–16.
9. Wang Z, Sun J, Yan J, Gao P, Zhang H, Yang Y, et al. Comparison of the efficacy of posterioranterior screws, anterior-posterior screws and a posterior-anterior plate in the fixation of posterior malleolar fractures with a fragment size of ≥ 15 and < 15%. BMC Musculoskelet. Disord. 2020; 21:570.
10. Stringfellow TD, Walters ST, Nash W, Ahluwalia R. Management of posterior malleolus fractures: A multicentre cohort study in the United Kingdom. Foot Ankle Surg. 2021; 27: 629–35.
11. Mason LW, Kaye A, Widnall J, Redfern J, Molloy A. Posterior malleolar ankle fractures: an effort at improving outcomes. JB JS Open Access 2019; 4(2):e0058.
12. Bergman C, Morin M, and Lawson K. Anatomy, Classification, and Management of Ankle Fractures Involving the Posterior Malleolar Fragment: A Literature Review. Foot Ankle Orthop. 2019; 4(4) 1-11.
13. Pina G, Fonseca F, Vaz A, Carvalho A, Borralho N. Unstable malleolar ankle fractures: evaluation of prognostic factors and sports return. Arch Orthop Trauma Surg 2021; 141:99–104. https://doi.org/10.1007/s00402-020-03650-w.
14. Tantigate D, Ho G, Kirschenbaum J et al. Functional outcomes after fracture- dislocation of the ankles. Foot Ankle Spec 2019; 13 (1):18-26.
15. Palmanovich E, Ohana N, Yaacobi E, Segal D, Iftach H, Sharfman ZT, et al. Preoperative planning and surgical technique for optimizing internal fixation of posterior malleolar fractures: CT versus standard radiographs. J Orthop Surg Res 2020; 15:119.
16. Yearson D , Melendez I , Anain F , Siniscalchi S , Drago J. Posterior malleolar fractures. New classification and treatment algorithm. J Foot Ankle. 2020; 14(3):254-9.
17. Kang C, Hwang D, Lee J, Won Y, Song J, Lee G. Screw fixation of the posterior malleolus fragment in ankle fracture. Foot Ankle Int 2019 ;40(11):1288–94.
18. Han SM, Wu TH, Wen JX, Wang Y, Cao L, Wu WJ, et al. Radiographic analysis of adult ankle fractures using combined Danis-Weber and Lauge-Hansen classification systems. Scientific Reports 2020; 10:7655. https://doi.org/10.1038/s41598-020-64479-2.
19. Tosun B, Selek O, Gok U, Ceylan H. Posterior malleolus fractures in Trimalleolar ankle fractures: malleolus versus Transyndesmal fixation. Indian J Orthop. 2018; 52(3):309–14.
20. Kumar A, Mishra P, Tandon A, Arora R, Chadha M. Effect of CT on management plan in malleolar ankle fractures. Foot Ankle Int 2018 ; 39(1):59–66.
21. Rammelt S, Bartonicek J . Posterior malleolar fractures: J. Crit. Rev. JBJS Rev 2020 ; 8(8):e19.
22. Sultan F, Zheng X, Pan Z, Zheng Q, Li H, Wang J . Characteristics of intercalary fragment in posterior malleolus fractures. Foot Ankle Surg 2020; 26(3):289–94.

To Cite:

El Sammak, D, Alsowey, A., khamis, M., Can MSCT be a Useful Tool to Orthopedic Surgeons in Assessment of The Morphology of The PM (Posterior Malleolus) Fractures Using Bartonicek-Rammelt Classification? *Zagazig University Medical Journal*, 2023; (257-265): -.doi: 10.21608/zumj.2022.155920.2621.